Research on Control System of Three-Phase Isolated AC/DC Converter

Xiang Ao and Zhihao Jia

Abstract The isolated AC/DC converter has many advantages such as the ability to convert electricity according to needs, high efficiency, small size, high power density, and the ability to act as a load or power source on demand. The corresponding modulation strategy and control strategy of the topology are analyzed in this paper. Due to the impact of the peak inductance current in its topology on system performance, this paper proposes a control strategy for minimizing the peak value of inductance current to improve system reliability and reduce on-state losses. The optimal algorithm is used to simultaneously change the modulation coefficient and external phase angle to achieve the minimum peak value of inductance current, and the experimental results verify proposed method.

Keywords AC/DC converter · Matrix converter · Control strategy · Peak value of inductance current

1 Introduction

In the recent years, the three-phase isolated AC-DC converter has been proposed as a converter between AC grid and DC power source or load [1–4]. Because of high efficiency, high power density, and bi-directional power transfer ability, the topology has enormous application prospects.

After studying traditional control methods such as direct current control with fixed external phase angle, direct current control with fixed modulation coefficient, and model prediction with fixed modulation coefficient, it was found that the above traditional methods are either constant modulation coefficient or constant phase angle control, which cannot achieve control of the peak value of inductance current.

X. Ao (✉) · Z. Jia
North China University of Technology, Beijing, China
e-mail: 313849963@qq.com

S. Yadav et al. (eds.), *Energy Power and Automation Engineering*, Lecture Notes in Electrical Engineering 1118, https://doi.org/10.1007/978-981-99-8878-5_43

This paper proposed a coordinated optimal control algorithm based on the minimum modulation coefficient and external phase angle of the peak value of inductance current. By changing the modulation coefficient and external phase angle simultaneously through the optimal algorithm, the peak value of inductance current of the isolated AC/DC converter is minimized, the on-state loss of the device is reduced, and the system efficiency and steady-state performance are improved. Based on the above optimal algorithm, this paper proposes two control strategies: the minimum PI control strategy for the peak value of inductance current and the minimum model predictive control strategy for the peak value of inductance current. Finally, the proposed method was validated using MATLAB/Simulink and an experimental platform.

2 System Topological Structure and Working Principle

2.1 System Topology

The circuit topology of the isolated AC/DC matrix converter (IAMC) is shown in Fig. 1, from left to right, consisting of a three-phase AC power supply, grid-side filter, 3–1 matrix converter, high-frequency transformer, rear stage H-bridge circuit, DC side filter, and load [5, 6].

In Fig. 1, u_{sa}, u_{sb}, and u_{sc} are three-phase AC voltages, i_{sa}, i_{sb}, and i_{sc} are grid-side currents, u_a, u_b, and u_c are the three-phase input voltages of the 3–1 matrix converter, and the currents are i_a, i_b, and i_c. The output voltages of the 3–1 matrix converter are u_p, and the current is i_L. The output voltages of the high-frequency transformer are u_s. i_{dc} is the load side current and u_0 is the load side voltage [7].

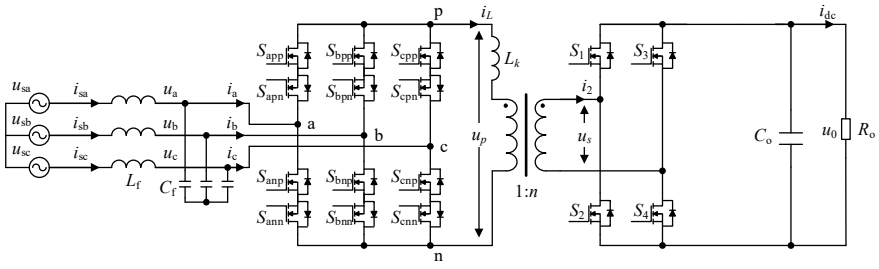

Fig. 1 IAMC main circuit topology

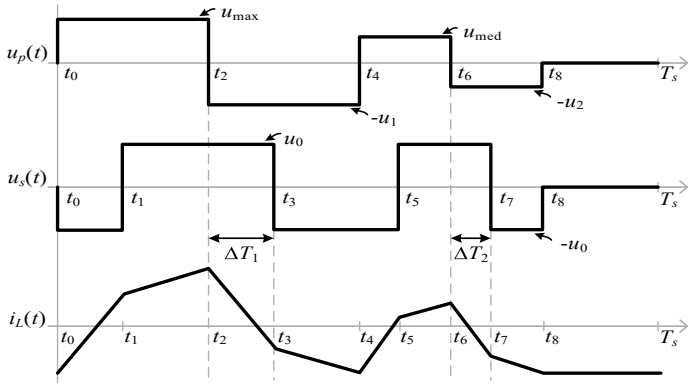

Fig. 2 Waveform of voltage and inductive current at both ends of transformer

2.2 Modulation Strategy of IAMC Circuit

The front stage 3–1 matrix converter adopts a bipolar current space vector modulation strategy. The input of the front stage 3–1 matrix converter is an AC voltage source. During circuit operation, the AC power supply cannot be short circuited, and a free moving path needs to be provided for the inductor L_k. In order to ensure its normal operation, the upper and lower bridge arms of the front stage 3–1 matrix converter can only conduct one bi-directional switch at any time [8–11].

This paper divides a loop into 12 sectors, and the current reference current can be composed of two adjacent fundamental vectors and a zero vector.

To transmit power, a coordinated control method is used, which inserts a phase shift angle between the front stage 3–1 matrix converter and the rear stage H-bridge circuit. The voltage and current waveforms of the output voltage up of the front stage 3–1 matrix converter and the output voltage us of the rear stage H-bridge in one control cycle T_s are shown in Fig. 2.

Starting from t_0, the output voltage up of the previous stage 3–1 matrix converter divides a control cycle T_s into five time periods. The forward maximum line voltage $u_{\max}$ of the previous stage 3–1 matrix converter corresponds to the vector action time t_0–t_2, the forward minor line voltage u_{med} corresponds to the vector action time t_4–t_6, the negative maximum line voltage $u_{\max}$ corresponds to the vector action time t_2–t_4, and the negative minor line voltage u_{med} corresponds to the vector action time t_6–t_8, zero vector action time $t_8 - T_s$.

Divide a control cycle T_s into 9 time periods to obtain the timing of each control period: $t_1 = \Delta T_1$, $t_2 = \frac{d_1}{2}T_s$, $t_3 = \frac{d_1}{2}T_s + \Delta T_1$, $t_4 = d_1 T_s$, $t_5 = d_1 T_s + \Delta T_2$, $t_6 = d_1 T_s + \frac{d_2}{2}T_s$, $t_7 = d_1 T_s + \frac{d_2}{2}T_s + \Delta T_2$ Among them, $T_s = \frac{2\pi}{\omega_s}$, the phase shift time between the front and rear stages is $\Delta T_1 = \frac{\phi d_1 T_s}{2\pi}$, and $\Delta T_2 = \frac{\phi d_2 T_s}{2\pi}$, where ϕ is the external phase shift angle and its value range $0 \le \phi \le \pi/2$.

Table 1 Expressions for d_1, d_2, and d_0 when obtaining 12 sectors

Sector number K	d_1	d_2	d_0
1, 3, 5, 7, 9, 11	$d_1 = m\sqrt{\sin\left(-\theta_i + \frac{\pi}{3}\right)}$	$d_2 = m\sqrt{\sin(\theta_i)}$	$d_0 = 1 - d_1 - d_2$
2, 4, 6, 8, 10, 12	$d_1 = m\sqrt{\sin\left(\theta_i + \frac{\pi}{6}\right)}$	$d_2 = m\sqrt{\sin\left(-\theta_i + \frac{\pi}{6}\right)}$	$d_0 = 1 - d_1 - d_2$

The expressions for $d1, d2$, and $d0$ when obtaining 12 sectors are given in Table 1.

The range of modulation coefficient m is $0 \leq m \leq 1/\sqrt{2}$ and the range of sector angle θ_i is $0 \leq \theta_i \leq \frac{\pi}{6}$.

3 Minimum Control of Peak Inductance Current in Isolated AC/DC Converter

The range of voltage regulation in this topology is large. From the grid-side line voltage of the front stage 3–1 matrix converter in Fig. 3, for different load side voltages u_0, the peak inductance current will occur in the following two situations.

When the maximum line voltage $u_{\max}$ is greater than the load side voltage nu_0, the peak of inductance current is obtained at point A and B in the first case. When the maximum line voltage $u_{\max}$ is less than the load side voltage nu_0, the peak of inductance current is obtained at point C and D in the second case.

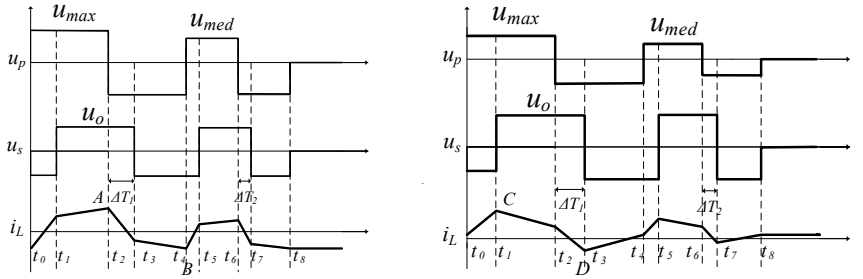

(a)Schematic diagram of inductance current in the first case

(b)Schematic diagram of inductive current in the second case

Fig. 3 Inductance current diagram

Take the first sector as an example, in the first case, the peak inductance current expression is:

$$\mathrm{i_{LAB}} = \frac{\delta d_1 T_s n u_o}{2L} - \frac{d_1 T_s n u_o}{2L} + \frac{d_1 T_s u_{\max}}{2L} \tag{1}$$

Formula for modulation factor m, phase shift angle ϕ, and current I_i as (2):

$$I_i = m^2 \frac{n u_0}{\omega_s L} \phi (1 - \frac{|\phi|}{\pi}) \tag{2}$$

When the reactive power is 0 and the current $I_\mathrm{i} = I_\mathrm{cd}, \phi = \delta\pi \,/\, 2$ will be substituted into Eq. (2), and then combined with Eq. (1) and Table 1 to obtain the expression (3) for the peak of the inductance current and shift ratio in the first sector:

$$i_{LAB} = -\frac{\sqrt{-\pi\delta n u_0(\delta-2)\omega_s L I_{cd}}\left(\sqrt{3}U_i\cos(\theta_i) + n(\delta-1)u_0\right)T_s\sqrt{\cos\left(\frac{\pi}{6}+\theta_i\right)}}{\pi\delta n u_0(\delta-2)L} \tag{3}$$

Take the derivative of expression (3), make its derivative function zero, and obtain its minimum in Eq. (4):

$$\delta = \frac{\left(\sqrt{3}U_i\cos(\theta_i) - n u_0\right)\sqrt{3}}{3U_i\cos(\theta_i)} \tag{4}$$

Similarly, the optimal shift corresponding to the minimum peak of the inductance current in the other 11 sectors can be obtained in two cases, as given in Table 2.

Table 2 Optimal shift corresponding to the minimum peak of the inductance current

Case	Sector	
	1, 3, 5, 7, 9, 11	2, 4, 6, 8, 10, 12
The first case (A, B)	$\delta = \frac{\left(\sqrt{3}U_i\cos(\theta_i) - n u_0\right)\sqrt{3}}{3U_i\cos(\theta_i)}$	$\delta = \frac{\left(\sqrt{3}U_i\sin(\frac{\pi}{3}+\theta_i) - n u_0\right)\sqrt{3}}{3U_i\sin(\frac{\pi}{3}+\theta_i)}$
The second case (C, D)	$\delta = -\frac{\sqrt{3}U_i\cos(\theta_i) - n u_0}{n u_0}$	$\delta = -\frac{\sqrt{3}U_i\sin(\frac{\pi}{3}+\theta_i) - n u_0}{n u_0}$

4 Simulink Results and Analysis

This paper uses MATLAB/Simulink to build a simulation model of an isolated AC/DC converter. The simulation results of constant modulation coefficient current direct control and model predictive control, inductance current peak minimum PI control, and model predictive control prove the correctness of the proposed control strategy. The main circuit parameters are given in Table 3.

The inductance current waveforms of the four control strategies are shown in Fig. 4.

Table 3 Parameters of IAMC

Description	Value	Description	Value
Input voltage U_i/V	40	Switching frequency f_s/kHz	20
AC side capacitor C_f/μF	92	Output side capacitance C_0/μF	800
AC side inductance L_f/μH	330	Reference voltage u_0^*/V	10
Transformer turn ratio n	1	Load resistance R/Ω	20

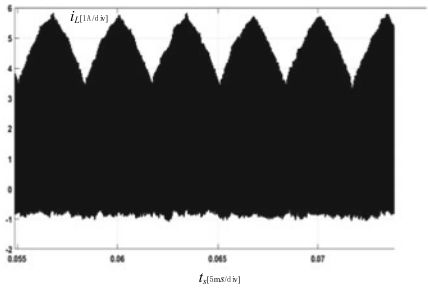

(a)PI control strategy for the minimizing peak inductance current

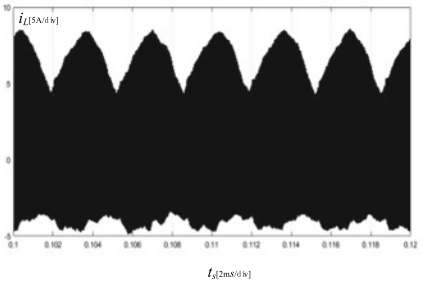

(b)Direct current control strategy with fixed modulation coefficient

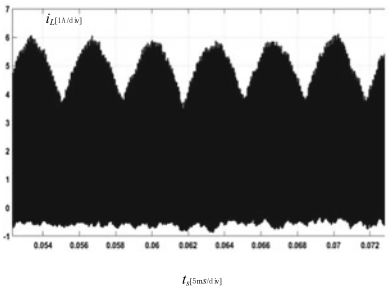

(c)MPC strategy for minimizing the peak inductance current

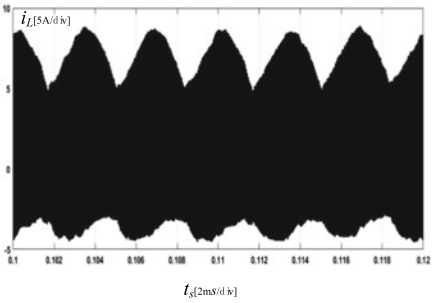

(d)MPC strategy with fixed modulation coefficient

Fig. 4 Inductive current waveform diagram

The simulation results of the relationship between peak inductance current, reference voltage, and load resistance of the four control strategies are shown in Figs. 5 and 6.

From the simulation results of Figs. 4, 5, and 6, the peak value of the inductance current of the proposed control strategy is smaller than that of the fixed modulation coefficient control strategy, which is consistent with theory.

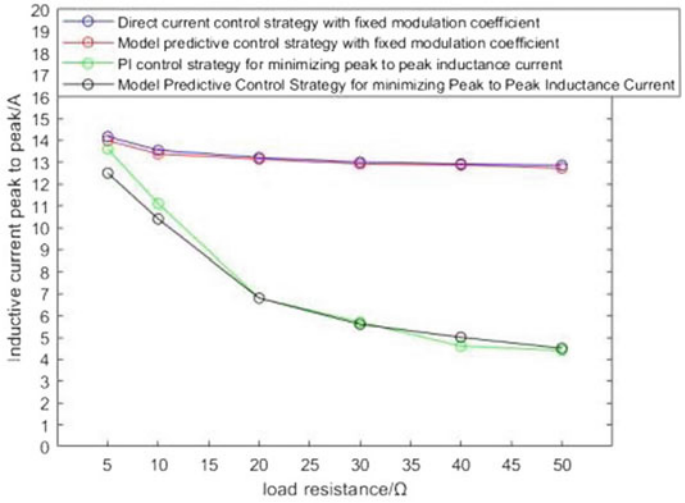

Fig. 5. Relationship between peak inductance current and load resistance

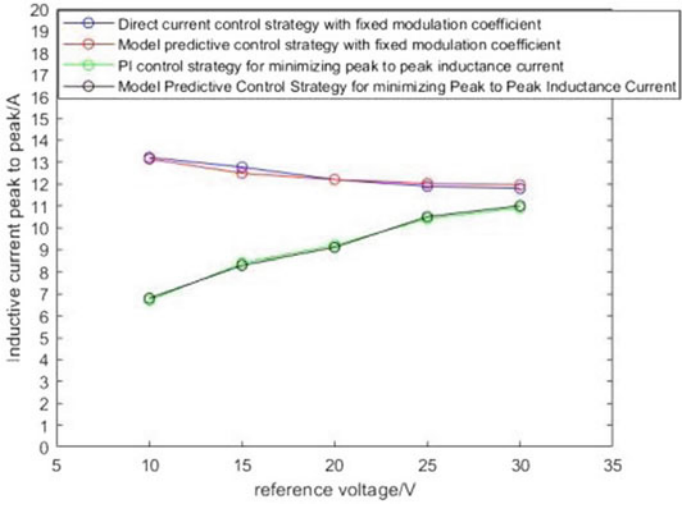

Fig. 6 Relationship between peak value of inductance current and reference voltage

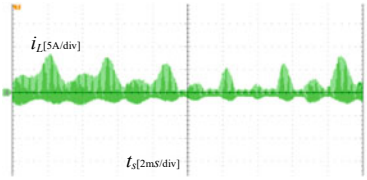

(a)PI control strategy for the minimizing peak inductance current

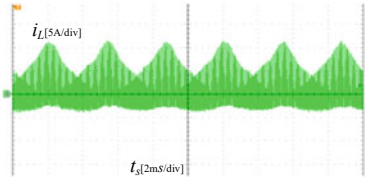

(b)Direct current control strategy with fixed modulation coefficient

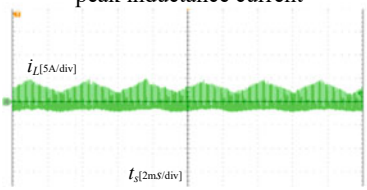

(c)MPC strategy for the minimizing peak inductance current

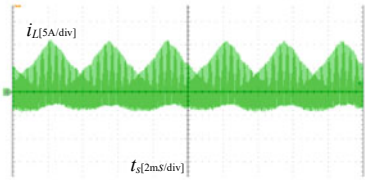

(d)MPC strategy with fixed modulation coefficient

Fig. 7 Inductive current waveform diagram

5 Experimental Results and Analysis

To further validate the effectiveness of this method through experiments, an experimental platform for the IAMC converter was established, and the experimental parameters were the same as the simulation parameters. The inductance current waveforms of the four control strategies are shown in Fig. 7.

The relationship between the peak of inductance current, reference voltage, and load resistance of the four control strategies is shown in Figs. 8 and 9.

From the experimental results in Figs. 7, 8, and 9, it can be observed that the peak value of the inductance current of the proposed control strategy is smaller than that of the fixed modulation coefficient control strategy, which is consistent with theory and simulation.

6 Conclusions

To achieve the minimum peak value of inductance current, this paper proposed a coordinated control method for modulation coefficient and external phase angle. The proposed method was compared with the conventional constant modulation coefficient control method in simulations and experiments. The results show that the proposed control strategy has the smallest peak inductance current with good dynamic performance.

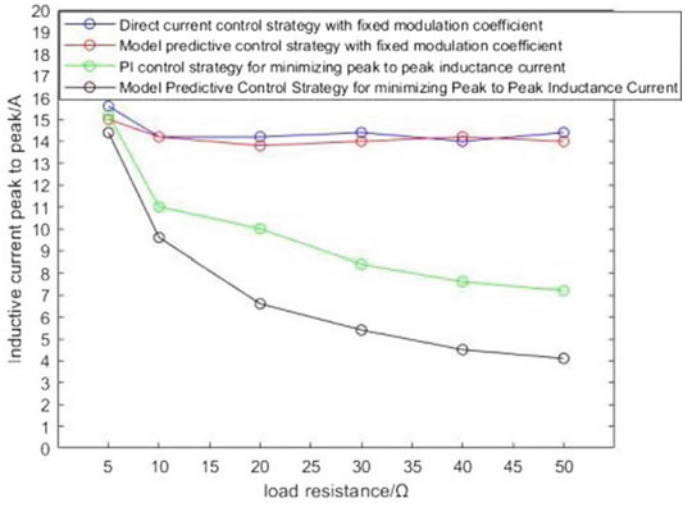

Fig. 8 Relationship between peak inductance current and load resistance

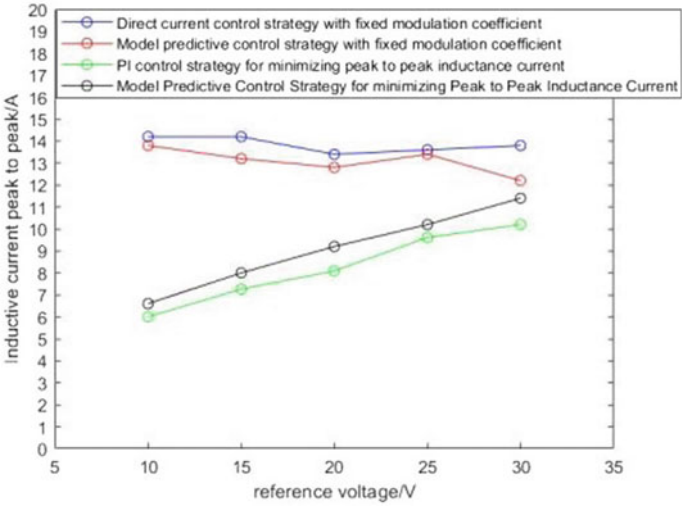

Fig. 9 Relationship between peak value of inductance current and reference voltage

References

1. Williamson SS, Rathore AK, Musavi F (2015) Industrial electronics for electric transportation: current state-of-the-art and future challenges. IEEE Trans Industr Electron 62(5):3021–3032
2. Song J, Zhao R, Kwasinski A (2011) Design considerations for energy storage power electronics interfaces for high penetration of renewable energy sources. ICPE (ISPE)

3. Vazquez S, Lukic SM, Galvan E et al (2010) Energy storage systems for transport and grid applications. IEEE Trans Industr Electron 57(12):3881–3895
4. Yilmaz M, Krein PT (2012) Review of battery charger topologies, charging power levels, and infrastructure for plug-in electric and hybrid vehicles. IEEE Trans Power Electron 28(5):2151–2169
5. Garcia-Gil R, Espi JM (2004) An all-digital controlled AC-DC matrix converter with high-frequency isolation and power factor correction. In: 2004 IEEE international symposium on industrial electronics. Istanbul, Turkey, IEEE, pp 1075–1080
6. García-Gil R, Espí JM, Dede EJ, et al (2005) A bidirectional and isolated three-phase rectifier with soft-switching operation. IEEE Trans Indus Electr 52(3):765–773
7. Singh AK, Das P, Panda SK (2014) Novel switching scheme for matrix based isolated three phase AC to DC conversion. In: IECON 2014-40th annual conference of the IEEE industrial electronics society. IEEE, pp 3324–3329
8. Varajao D, Araujo RE, Miranda LM et al (2018) Modulation strategy for a single-stage bidirectional and isolated AC-DC matrix converter for energy storage systems. IEEE Trans Industr Electron 65(4):3458–3468
9. Fang F, Li YW (2017) ModuLation and control method for bidirectional isolated AC/DC matrixbased converter in hybrid AC/DC microgrid. In: 2017 IEEE energy conversion congress and exposition (ECCE). IEEE
10. Shigeuchi K, Xu J, Shimosato N, Sato Y A new modulation method applying optimal duty cycle and phase shift for bidirectional isolated three-phase AC/DC converter based on matrix converter 3514–3521. https://doi.org/10.23919/IPEC.2018.8507521
11. Abdallah M, Suzuki K, Takeshita T, et al (2017) Soft-switching PWM technique for grid-tie isolated bidirectional DC-AC converter with Si C device. IEEE Trans Indus Appl 1–1